

COEXISTENCE OF RESONANT ACTIVATION  
AND NOISE ENHANCED STABILITY  
IN A MODEL OF TUMOR–HOST INTERACTION:  
STATISTICS OF EXTINCTION TIMES\*

ANNA OCHAB-MARCINEK<sup>†</sup>, EWA GUDOWSKA-NOWAK

Marian Smoluchowski Institute of Physics, Jagellonian University  
and Mark Kac Complex Systems Research Center  
Reymonta 4, 30–059 Kraków, Poland

ALESSANDRO FIASCONARO, BERNARDO SPAGNOLO

Dipartimento di Fisica e Tecnologie Relative and INFN-CNR  
Group of Interdisciplinary Physics<sup>‡</sup>, Università di Palermo  
Viale delle Scienze, 90128 Palermo, Italy

*(Received April 3, 2006)*

*Dedicated to Professor Peter Talkner on the occasion of his 60th birthday*

We study a Langevin equation derived from the Michaelis–Menten (MM) phenomenological scheme for catalysis accompanying a spontaneous replication of molecules, which may serve as a simple model of cell-mediated immune surveillance against cancer. We examine how two different and statistically independent sources of noise — dichotomous multiplicative noise and additive Gaussian white noise — influence the population’s extinction time. This quantity is identified as the mean first passage time of the system across the zero population state. We observe the effects of resonant activation (RA) and noise-enhanced stability (NES) and we report the evidence for competitive co-occurrence of both phenomena in a given regime of noise parameters. We discuss the statistics of first passage times in this regime and the role of different pseudo-potential profiles on the RA and NES phenomena. The RA/NES coexistence region brings an interesting interpretation for the growth kinetics of cancer cells population, as the NES effect enhancing the stability of the tumoral state becomes strongly reduced by the RA phenomenon.

PACS numbers: 05.40.–a, 82.20.–w, 05.10.–a

---

\* Presented at the XVIII Marian Smoluchowski Symposium on Statistical Physics, Zakopane, Poland, September 3–6, 2005.

<sup>†</sup> ochab@th.if.uj.edu.pl

<sup>‡</sup> <http://gip.dft.unipa.it>

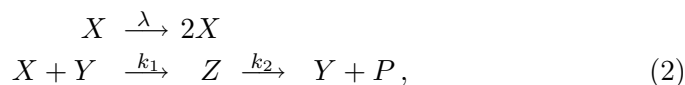
## 1. Introduction

Since the times of Delbrück [1], a considerable research has been done on auto-catalytic reactions using stochastic models [2,4]. Spontaneous random molecular fluctuations play a significant role in the driving kinetic mechanism of many regulatory enzymatic reactions. Random fluctuations in genetic networks are inevitable as chemical reactions are probabilistic and many genes, RNAs and proteins are present in low numbers per cell. Gene expressions, for example, involves a series of single-molecule events subject to significant thermal fluctuations, which may result in a divergence of fate and lead to non-genetic population heterogeneity. Moreover, mean levels of heterogeneity for the populations are ensured by regulatory factors that tune the spontaneous fluctuations. Although many examples of potentially noise-exploiting cellular processes have been discussed and documented in literature, how cells function and process information when the underlying molecular events are random still remains an open question [4,14]. Other cellular processes influenced by noise include ion-channel gating, neural firing, cytoskeleton dynamics and molecular motors [15,18].

Simulation schemes that model each individual reaction event can be computationally demanding [2] as the copy of the input and output molecules increases. Therefore, as an alternative way to account for molecular fluctuations in biochemical reactions is to assume that the time evolution of a species of interest is produced at an average rate  $f(x)$ , degraded at rate  $g(x)$  and follows the stochastic differential equation:

$$\frac{dx}{dt} = f(x) - g(x) + \xi(t). \quad (1)$$

In the above equation the noise term is appended as the additive (white) noise source  $\xi(t)$  weakly perturbing deterministic evolution of the system. Obviously, implicit for such a formulation is a continuous description of molecular species where the dynamics is cast in terms of infinitesimal changes of concentrations. Eq. (1) will be further postulated to study dynamics of a catalytic reaction. We consider the phenomenological Michaelis–Menten scheme for the catalysis accompanying a spontaneous replication of molecules



where a substrate  $X$  forms first a complex  $Z$  with molecules of the enzyme  $Y$ , before the conversion of  $X$  to a product  $P$  is completed. By assuming that the production of  $X$ -type molecules inhibited by a hyperbolic activation

(Michaelis–Menten inhibition kinetics) is the slowest process under consideration and by considering a conserved mass of enzymes  $Y + Z = E = \text{const}$ , the resulting kinetics can be recast in the form of the 1-dim Langevin equation

$$\frac{dx}{dt} = -\frac{dU(x)}{dx} + \xi(t), \tag{3}$$

with the pseudo–“free-energy” potential profile  $U(x)$  expressed as [19]

$$U(x) = -\frac{x^2}{2} + \frac{\theta x^3}{3} + \beta x - \beta \ln(x + 1), \tag{4}$$

where  $x$  is the normalized molecular density with respect to the maximum number of molecules, and with the following scaling relations

$$x = \frac{k_1 x}{k_2}, \quad \theta = \frac{k_2}{k_1}, \quad \beta = \frac{k_1}{\lambda}, \quad t = \lambda t. \tag{5}$$

The time-scale separation performed on a kinetic scheme of the system (2) requires that a subset of species is asymptotically at steady state on the time scale of interest, and is known as a quasi-steady-state assumption [4,5]. It reduces the model complexity by effectively reducing the number of considered molecular species and reactions.

In the case of Michaelis–Menten kinetics this approximation assumes also much larger concentration of substrate  $X$  than the enzyme concentration  $E$  and with the steady-state constraint  $dZ/dt = 0$  leads to a characteristic regulatory term  $-\beta x/(1 + x)$  in the dynamic (3). The resulting potential profile Eq. (4) has at most three extrema representing deterministic stationary states of the system (see Fig. 1)

$$x_1 = 0, \tag{6}$$

$$x_2 = \frac{1 - \theta + \sqrt{(1 + \theta)^2 - 4\beta\theta}}{2\theta}, \tag{7}$$

$$x_3 = \frac{1 - \theta - \sqrt{(1 + \theta)^2 - 4\beta\theta}}{2\theta}. \tag{8}$$

The essential feature captured by the model is, for a constant parameter  $\theta$ , the  $\beta$ -dependent bistability. In the above form and by assuming time dependent, random variations of the parameter  $\beta$ , the model has been used to describe an effect of cell-mediated immune surveillance against the cancer [20]. Most of tumoral cells bear antigens which are recognized as strange by the immune system. A response against these antigens may be mediated either by immune cells such as T-lymphocytes or other cells, not directly

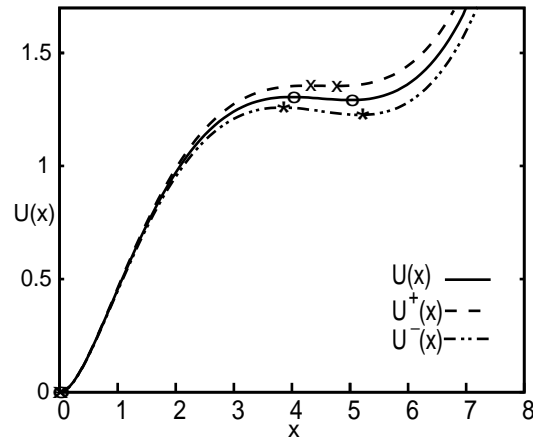


Fig. 1. The Michaelis–Menten potential with parameters:  $\beta = 3$ ,  $\theta = 0.1$ ,  $\Delta = 0.02$ . Labels: “o”: extrema of  $U(x)$ :  $x = 0, 4, 5$ ; “x”: extrema of  $U^+(x)$ :  $x = 0, 4.28, 4.72$ ; “\*”: extrema of  $U^-(x)$ :  $x = 0, 3.83, 5.17$ .

related to the immune system (like macrophages or natural killer cells). The process of damage to tumor proceeds via infiltration of the latter by the specialized cells which subsequently develop a cytotoxic activity against the cancer cell-population. The series of cytotoxic reactions between the cytotoxic cells and the tumor tissue may be considered to be well approximated by a saturating, enzymatic-like process whose time evolution equations are similar to the standard Michaelis–Menten kinetics. The variability of kinetic parameters defining this process naturally affects the extinction of the tumor [20, 21].

The process of population growth and decay can be described as a motion of a fictitious particle in a potential  $U(x)$ , whose shape varies in time due to the noisy  $\beta$  parameter. Minima of the potential correspond to stable states of the population, where, in case of a purely deterministic system, the cell concentration does not grow or decay. One of the minima is always at  $x = 0$ , which reflects the fact that the state in which cancer cells are absent is a stable one. The other minimum corresponds to a fixed-size cell population. Noise-induced transition between those stable states across the potential barrier may be interpreted as a “spontaneous” extinction of cancer due to environmental fluctuations, as well as due to random variations in the immune response efficiency. We will study a system with parameters chosen in such a way that  $x = 0$  is a global minimum. We are interested in the lifetime of the metastable state. Mean escape time has been intensively studied in order to characterize the lifetime of metastable states of static and fluctuating potentials with different initial conditions [22, 41]. The studies

show that the mean escape time has different non-monotonic behaviors as a function of both the thermal noise intensity and the mean frequency of potential fluctuations. These behaviors are a signature of two noise-induced effects, namely the resonant activation (RA) [22, 33] and the noise enhanced stability (NES) [34, 41]. The NES effect increases the average lifetime of the metastable state, while the RA phenomenon minimizes this lifetime.

The purpose of this work is to find the optimal range of parameters in which the positive role of resonant activation phenomenon, with respect to the cancer extinction, prevails over the negative role of NES, which enhances the stability of the tumoral state. The following section explains more extensively the concepts of resonant activation and noise-enhanced stability and their role in the analysis of cancer growth kinetics. In the next section we report the appearance of RA and NES phenomena in this model and we discuss the statistics of first passage times in this regime. In the same section the role of different potential profiles on the RA and NES effects, with piece-wise linear and MM potentials with reflecting boundary is analyzed. Finally we draw the conclusions.

## 2. The model system

### 2.1. Mean first passage time analysis

Our starting point is the Langevin equation of an overdamped Brownian particle moving in a random fluctuating potential barrier

$$\frac{dx}{dt} = -\frac{dV(x,t)}{dx} + \xi(t),$$

$$V(x,t) = U(x) + G(x)\eta(t). \tag{9}$$

Here  $\xi(t)$  is a Gaussian process with zero mean and correlation function  $\langle \xi(t)\xi(t') \rangle = \sigma^2\delta(t-t')$ . The potential  $V(x,t)$  is the sum of two terms: the fixed potential  $U(x)$  and the randomly switching term  $G(x)\eta(t)$ , where  $\eta(t)$  stands for a Markovian dichotomous noise switching between two levels  $\{\Delta^+, \Delta^-\}$ , where  $\Delta^+ = \Delta$  and  $\Delta^- = -\Delta$ . The probability of switching ( $\pm\Delta \rightarrow \mp\Delta$ ) per time unit, or the mean frequency of switching, is labelled  $\nu = 1/(2\tau)$ , and the autocorrelation function of the dichotomous noise yields

$$\langle (\eta(t) - \langle \eta \rangle)(\eta(t') - \langle \eta \rangle) \rangle = \frac{(\Delta^+ - \Delta^-)^2}{4} e^{-|t-t'|/\tau}.$$

The two noise sources are statistically independent, *i.e.*  $\langle \xi(t)\eta(s) \rangle = 0$ . The potential  $V(x,t)$ , therefore, flips at random time between two configurations

$$U^\pm(x) = U(x) + G(x)\Delta^\pm. \tag{10}$$

The corresponding Fokker–Planck equations which describe the evolution of probability density of finding the state variable in a “position”  $x$  at time  $t$  are

$$\begin{aligned} \partial_t p(x, \Delta^\pm, t) &= \partial_x \left[ \frac{dU^\pm(x)}{dx} + \frac{1}{2}\sigma^2 \partial_x \right] p(x, \Delta^\pm, t) \\ &\quad - \frac{1}{2\tau} p(x, \Delta^\pm, t) + \frac{1}{2\tau} p(x, \Delta^\mp, t). \end{aligned} \quad (11)$$

In the above equations time has dimension of  $[length]^2/energy$  due to a friction constant that has been “absorbed” in a time variable. With the initial condition

$$p(U^\pm, x_s, t)|_{t=0} = \frac{1}{2}\delta(x - x_s), \quad (12)$$

from Eq. (11) we get the equations for the mean first passage times (MFPTs):

$$\begin{aligned} -1 &= -\frac{T^+(x)}{\tau} + \frac{T^-(x)}{\tau} - 2 \frac{dU^+(x)}{dx} \frac{dT^+(x)}{dx} + \sigma^2 \frac{d^2 T^+(x)}{dx^2}, \\ -1 &= \frac{T^+(x)}{\tau} - \frac{T^-(x)}{\tau} - 2 \frac{dU^-(x)}{dx} \frac{dT^-(x)}{dx} + \sigma^2 \frac{d^2 T^-(x)}{dx^2}, \end{aligned} \quad (13)$$

where  $T^+(x)$  and  $T^-(x)$  denote MFPT for  $U^+(x)$  and  $U^-(x)$ , respectively. The overall MFPT for the system is derived from the above set of equations  $T(x) = T^+(x) + T^-(x)$  by assuming a reflecting boundary condition at  $x = a$  and an absorbing boundary at  $x = b$ :

$$\begin{aligned} \left. \frac{dT^\pm(x)}{dx} \right|_{x=a} &= 0, \\ T^\pm(x)|_{x=b} &= 0. \end{aligned} \quad (14)$$

Analytical solutions of Eqs. (13) can be expressed in a compact form only for piece-wise linear or piece-wise constant potentials [22, 23]. More complex cases require either use of approximation schemes [26, 28, 29], perturbative approach [27], or direct numerical evaluation methods [25, 31, 32].

## 2.2. Resonant activation

The signature of the resonant activation phenomenon is the occurrence of a minimum of the MFPT as a function of the mean frequency of the switching  $\nu$  of the multiplicative dichotomous noise. As a consequence the resonant activation effect minimizes the average lifetime of a population in the metastable state. Let us assume that the Brownian particle is behind

the potential barrier, in a neighborhood of the metastable state. When the barrier fluctuations are very fast the particle “sees” the average potential between the higher and lower configurations. The MFPT will tend to a constant value corresponding to the average static potential

$$\lim_{\tau \rightarrow 0} \text{MFPT}(U^+, U^-, \tau) = \text{MFPT} \left( \frac{U^+}{2} + \frac{U^-}{2} \right). \quad (15)$$

If the barrier fluctuations are slower than the actual escape rate ( $\tau$  large), the particle will escape before any barrier flip occurs. Therefore, the mean first passage time also tends to a constant, which now will be an average of the escape times for the higher and lower configurations of the potential

$$\lim_{\tau \rightarrow \infty} \text{MFPT}(U^+, U^-, \tau) = \frac{1}{2} [\text{MFPT}(U^+) + \text{MFPT}(U^-)]. \quad (16)$$

If the potential barrier is high enough or the additive noise is weak enough, the mean first passage time in a static potential can be approximated by the inverse of the Kramers escape rate, which increases exponentially with  $\Delta U(x)/\sigma^2$ , where  $\Delta U(x)$  is the height of the barrier. Such an exponential dependence guarantees the existence of a minimum of MFPT ( $\tau$ ). Its value at intermediate  $\tau$  is lower than both asymptotic mean first passage times, for very large or very small  $\tau$  [30]. Specifically, the MFPT at very low mean switching frequency (Eq. (16)) will be higher than the MFPT at the high frequency limit (Eq. (15)). In the middle frequency regime the effective escape rate over the fluctuating barrier is the average of the escape rates

$$K_{\text{eff}} = \frac{1}{2} (K_+ + K_-), \quad (17)$$

where  $K_+ = 1/\text{MFPT}(U^+)$  and  $K_- = 1/\text{MFPT}(U^-)$ , with  $K_- \ll K_+$ . Because of the exponential dependence, the MFPT in this intermediate frequency regime will be smaller than both  $\text{MFPT}_{\tau \rightarrow \infty}$  and  $\text{MFPT}_{\tau \rightarrow 0}$ .

### *2.3. Noise-enhanced stability*

The signature of the noise-enhanced stability effect is the occurrence of a maximum of the MFPT as a function of the additive noise intensity, for a fixed mean frequency  $\nu$  of the multiplicative noise. As a consequence the NES effect, differently from the RA phenomenon, maximizes the average lifetime of the population in the metastable state. The non-monotonic behavior of the mean escape time as a function of the additive noise intensity  $\sigma$  depends on the potential profile parameters, on the parameters of the multiplicative dichotomous noise and also on the initial position of the Brownian

particle [35, 38]. Noise enhances the stability of the metastable state with different peculiarities related to different dynamical regimes: the average lifetime can greatly increase when the noise intensity is very low with respect to the height of the barrier and the initial positions of the Brownian particles are in the “divergent” dynamical regime [41, 44]. When the particle starts from initial positions within the potential well, at small values of  $\sigma$  with respect to the height of the potential barrier and for a fixed potential, it will follow the monotonic behavior of the Kramers formula, as a function of the noise intensity. The mean escape time will then tend to infinity for  $\sigma \rightarrow 0$ . If the particle starts from outside the well, at small  $\sigma$  it will at once run down from its starting region towards the absorbing barrier and its mean escape time will be approximately equal to the escape time of a deterministic particle. At high noise intensities, the mean escape time decreases monotonically, regardless of initial positions. At intermediate noise intensities, a particle starting from the outer slope may sometimes be trapped into the well. Such events, although rare, can significantly increase the mean escape time because a trapped particle stays then in the well for a relatively long time.

#### 2.4. Population model

The kinetics of our biological system is described by the equation

$$\frac{dx}{dt} = (1 - \theta x)x - \beta \frac{x}{x + 1}, \quad (18)$$

where  $x(t)$  is the concentration of the cancer cells. The profile of the corresponding quasi-potential (Eq. (4)) presents a double well with one of the minima at  $x = 0$ . The region for  $x > 0$  can show either a monotonic behavior or a local minimum, depending on the values of parameters  $\theta$  and  $\beta$ . In the present investigation we used only parameters able to give a local minimum of the Michaelis–Menten potential for  $x > 0$ :  $\theta = 0.1$  and  $\beta = 3$  (see Fig. 1). For  $x \rightarrow \infty$  the potential shows a strong cubic repulsion. Our biological system is an open system whose random interactions with the environment and the random fluctuations of the immune system are described by an additive noise term  $\sigma\xi(t)$  in Eq. (18), and a dichotomous Markovian noise  $\eta(t)$ , of amplitude  $\Delta$  and mean correlation time  $\tau$  in the  $\beta$  parameter. As a consequence the stochastic Michaelis–Menten potential switches between two conformational states  $U^\pm(x)$

$$U^\pm(x) = -\frac{x^2}{2} + \frac{\theta x^3}{3} + (\beta \pm \Delta)(x - \ln(x + 1)), \quad (19)$$

and the Langevin equations for the system are

$$\begin{aligned} \dot{x} &= -\frac{dU^\pm(x)}{dx} + \xi(t) \\ &= x(1 - \theta x) - (\beta \pm \Delta)\frac{x}{x + 1} + \xi(t). \end{aligned} \tag{20}$$

The process of population growth and decay can be described as a motion of a fictitious particle in the switching potential between two configurations  $U^+(x)$  and  $U^-(x)$ . For negligible additive noise and small concentration of cancerous cells, this model resembles a standard Verhulst equation with perturbing multiplicative dichotomous noise, which exhibits a complex scenario of noise-induced transitions, observable in a pattern of the stationary probability density [42]. Here, we will address kinetic properties of this model by studying the mean first passage time between high and low population states in the system. We will study how the two different sources of noise as well as the position of the starting point  $x_{\text{in}}$  influence the mean first passage time. We put the absorbing boundary at  $x = 0$  and the reflecting one at  $x = \infty$ . The event of passing through the absorbing boundary is equivalent to a total extinction of cancer.

### 3. Results

#### *3.1. Michaelis–Menten and piece-wise linear potentials with absorbing boundary*

Here we analyze the role of different potential profiles with a reflecting barrier placed on the minimum of the fixed MM potential, that is in absence of dichotomous noise. We consider two cases: (i) MM potential, and (ii) piece-wise linear potential. Both cases are approximations of the effective MM potential (Fig. 1). Particularly the piece-wise linear potential is a good theoretical model, which enables us to obtain closed analytical expressions for the MFPT (see Refs. [22, 23]). In Fig. 2 we present the results of simulations on both cases and compare the behaviors of MFPT for NES and RA phenomena with those obtained using the exact MM potential profile (see Fig. 1). The NES effect, for a fixed value of the correlation time of the multiplicative noise and an unstable initial position, is shown in Fig. 2(a). The reflecting barrier placed in the proximity of the metastable state pushes the particle away from it and, therefore, decreases the MFPT for all values of the noise intensity, producing an overall reduction of the NES effect. The Brownian particle experiences only two different slopes in the piece-wise linear potential, while many more slopes are experienced and, therefore, more time is spent by it around the metastable state in the MM potential [35].

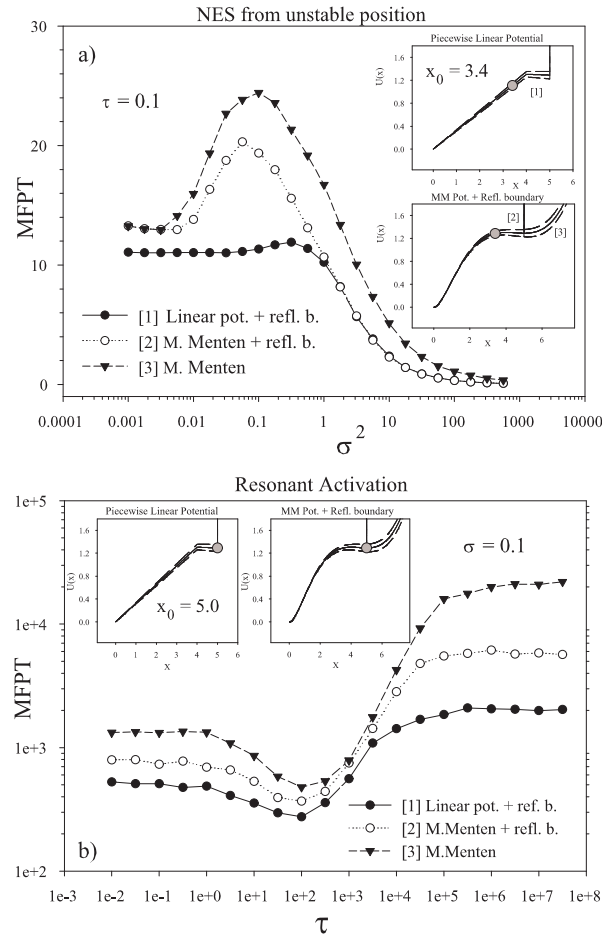


Fig. 2. (a) MFPT as a function of the additive noise intensity  $\sigma^2$  for three potential profiles: [1] piece-wise linear with a reflecting boundary, with slopes  $k_1 = +0.32$  and  $k_2 = -0.025$  in the average position; [2] Michaelis–Menten (MM) with a reflecting boundary; [3] exact MM potential. The unstable initial position is at  $x_0 = 3.4$  and  $\tau = 0.1$ . (b) MFPT as a function of the correlation time of the multiplicative noise. The initial position is  $x_0 = 0.1$ ,  $\sigma = 0.1$  and the number of realizations is  $N = 10^4$ . All the other potential parameters are the same as in Fig. 1.

That explains why the piece-wise linear potential is the worst approximation among all potential schemes. For noise intensity values greater than the height of the potential barrier, the different shape of the potential profile becomes irrelevant and the decreasing of MFPT values is due to the reflecting boundary only. In Fig. 2(b) the MFPT as a function of the correlation time of the multiplicative noise is presented, at a fixed value of the noise

intensity and for various approximations to the MM potential profile. The effect of the reflecting boundary is again to decrease all the MFPT values in the MM potential and, therefore, to reduce the absolute values of the RA phenomenon. The minimum of MFPT is, of course, more pronounced in the exact MM potential and the piece-wise linear potential is again the worst approximation. Both effects are robust enough to be observed in different potential profiles.

*3.2. Coexistence of noise-enhanced stability and resonant activation*

In this section we look for the coexistence region of RA and NES effects. We calculate, therefore, the MFPT for the following initial positions  $x_{in} = 3, 3.65, 5$ . We performed a series of Monte Carlo simulations of the stochastic process (20) with an absorbing boundary at  $x = 0$ , natural reflecting boundary at  $x = +\infty$  and the values of parameters:  $\beta = 3, \theta = 0.1, \Delta = \pm 0.02$ . The statistics for each MFPT has been taken from  $N = 10^4$  (for  $x_{in} = 3.65$ ) and  $N = 10^3$  (for  $x_{in} = 3$  and 5) simulation runs. The results reported here are an extension of those presented in [43]. The results confirm the existence of resonant activation and noise-enhanced stability phenomena in the studied system. Moreover, we have shown that in a certain range of parameters both effects can occur together [38–40].

In Figs. 3 and 4 we present the combined view of RA and NES effects. The considerations of subsection 2.2 are valid not only for trajectories starting from inside the potential well, but also for arbitrary initial positions in the potential, if only the particle has a chance to be trapped behind the potential barrier for some time. If the additive noise intensity is very large, a particle starting from the outer slope of the barrier does not “feel”

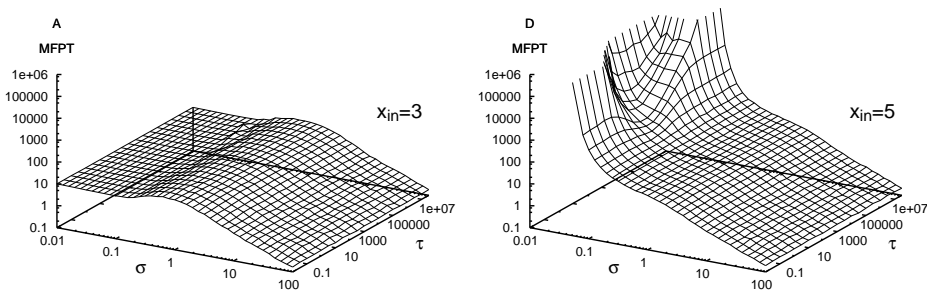


Fig. 3. MFPT as a function of the additive noise intensity  $\sigma$  and the correlation time of multiplicative noise. Initial positions:  $x_{in} = 3$  (left panel),  $x_{in} = 5$  (right panel). Parameters:  $\beta = 3, \theta = 0.1, \Delta = \pm 0.02$ . Number of simulation runs per each point:  $N = 10^3$ .

the barrier at all. If, in turn, the additive noise is very weak, the particle slides down the slope in an almost deterministic way. But at intermediate values of  $\sigma$ , the particle can (in some, very infrequent, realizations of the stochastic process) be trapped behind the barrier and, in case of such a rare event, its escape time changes non-monotonically as a function of  $\tau$ , in a way described in subsection 2.2. This effect of coexistence of noise-enhanced stability and resonant activation effects can be observed in Fig. 4. When the trajectory starts on the outer slope of the potential, only small fraction of the realizations are trapped into the well, and thus the RA effect is very small because only few trajectories will contribute to it. In order to obtain a well-visible RA (a large enough number of trapped trajectories) we have to choose the initial position sufficiently close to the top of  $U^-(x)$ . We have chosen  $x_{\text{in}} = 3.65$ . For this initial position we observe a co-occurrence of NES and RA. Since both effects act here in an opposite way, there exists a regime of  $\sigma$  and  $\tau$  parameters where noise-enhanced stability is strongly reduced by resonant activation. This region is well visible in Fig. 4 for values of parameters:  $\sigma \approx 0.06$ ,  $\tau \approx 100$ .

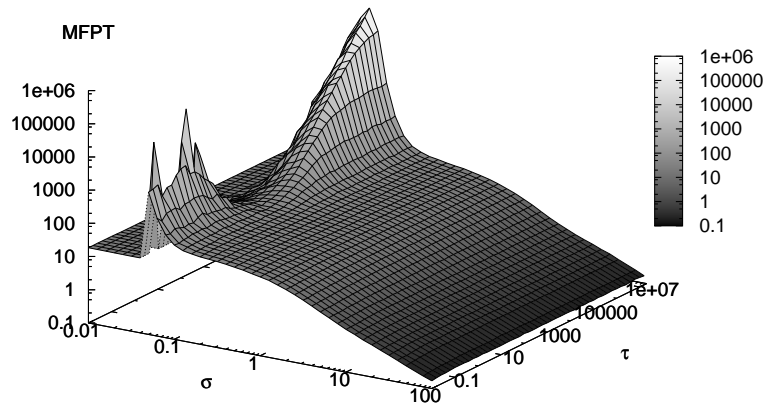


Fig. 4. MFPT as a function of the additive noise intensity  $\sigma$  and the correlation time of multiplicative noise. Initial position:  $x_{\text{in}} = 3.65$ . The parameters are the same as in Fig. 3. Number of simulation runs per each point:  $N = 10^4$ .

In Fig. 5 we present cross-sections of Fig. 4 at chosen values of  $\sigma$  and histograms of the first passage times corresponding to each point on the graphs. Most trajectories (more than 90% of all) are those which do not fall into the potential well. The trajectories trapped are minor contributions: their fraction (of the order of 0.1, 0.01 and even 0.001) depends on the barrier switching rate and on the additive noise strength. At  $0.01 < \sigma < 1$ , the first passage times of particles, which had not been trapped into the well, are of the order of 10. The first passage times of the trajectories trapped behind the potential barrier depend, of course, on  $\tau$ : In the region where

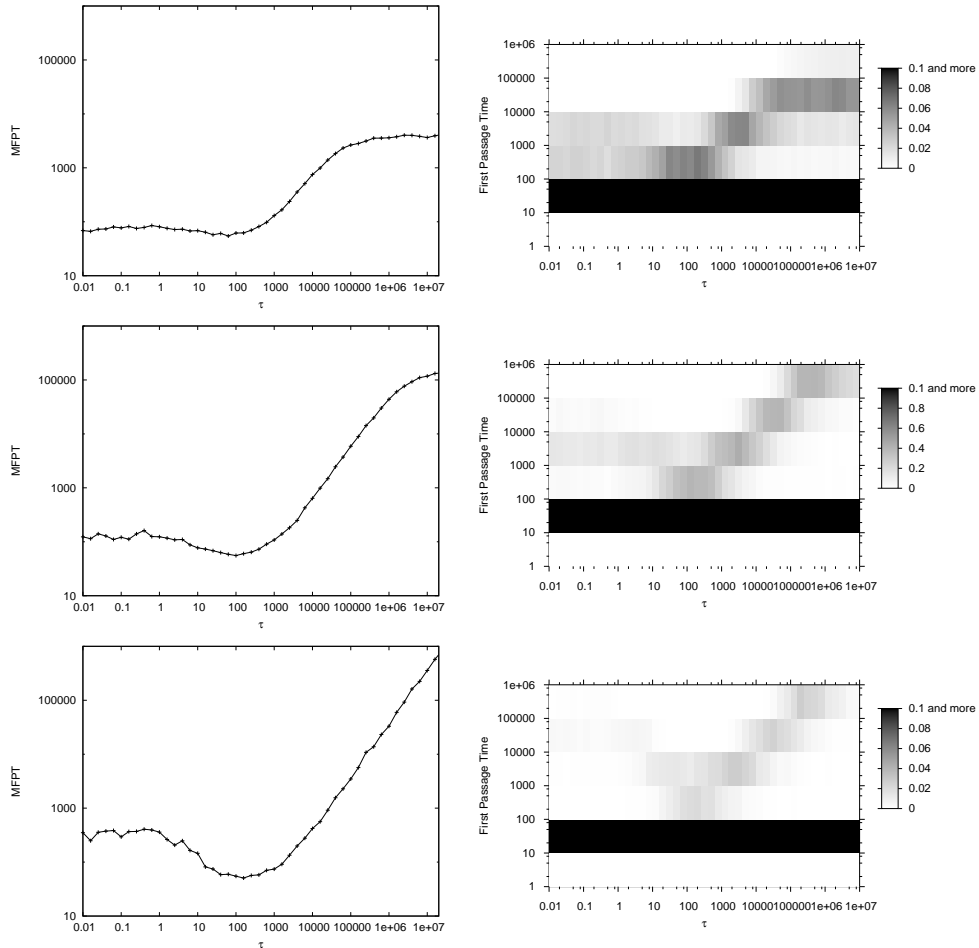


Fig. 5. Left panels: MFPT as a function of  $\tau$  for chosen values of  $\sigma$  in the noise-enhanced stability regime. From top to bottom:  $\sigma = 0.10$ ,  $\sigma = 0.08$ ,  $\sigma = 0.06$ . Right panels: Corresponding first passage time histograms. Colors from white to black denote a fraction of all trajectories. Black color denotes values from 0.1 to 1. Initial position:  $x_{in} = 3.65$ . The other parameters are the same as in Fig. 3.

the resonant activation is better visible, for small  $\tau$  the first passage times are of the order of  $10^3$ , for large  $\tau$  they are of the order of  $10^6$  and more, and for the intermediate values of  $\tau$  the first passage time drops down to the order of  $10^2$ .

#### 4. Conclusions

We studied a Langevin equation derived from the phenomenological Michaelis–Menten scheme for catalysis accompanying a spontaneous replication of molecules. It contains an additive noise term (Gaussian white noise) and a multiplicative noisy driving (dichotomous noise) in the term responsible for inhibition of population growth. The models of that type are widely used in biophysical description of cell-mediated immune surveillance against cancer [19–21, 46, 47], analysis of cell survival including repair kinetics after exposure to ionizing radiation [45] or delineation of factors responsible for the efficient action of biological regulatory networks [4, 5, 9, 11]. We examined how the two different sources of noise influence the population's extinction time, identified with the mean first passage time of the system over the zero population state. We observe appearance of two noise-induced resonant phenomena in the system: Mean first passage time displays here a non-monotonic behavior which depends on the characteristic parameters of the noises present in the system, namely the additive noise intensity  $\sigma$  and the correlation time  $\tau$  of the multiplicative noise. The occurrence of a minimum in MFPT (resonant activation) is related to the  $\tau$  parameter, whereas the emergence of the maximum in MFPT (noise-enhanced stability) is connected with  $\sigma$ . We report the evidence for co-occurrence of resonant activation and noise-enhanced stability in the same regime of noise parameters. We observe that the strong stability enhancement of the metastable state comes from very few contributions from the trajectories trapped in it. Their first passage times are several orders of magnitude longer than the first passage times of the trajectories which approached the absorbing boundary without being trapped in the metastable state. We analyzed the role of different potential profiles, with a reflecting barrier, on RA and NES phenomena. We found a very interesting, from the point of view of growth kinetics of cancer cells, coexistence region of both effects. In this region the NES effect, which enhances the stability of the tumoral state, is strongly reduced by the RA effect, which enhances the cancer extinction. In other words, an asymptotic regression to the zero tumor size may be induced by controlling the noise affecting hyperbolic inhibition of a spontaneous proliferation of cells.

This work was supported by the European Science Foundation STOCH-DYN grant, MIUR and INFM-CNR.

#### REFERENCES

- [1] M. Delbrück, *J. Chem. Phys.* **8**, 120 (1940).
- [2] D.T. Gillespie, *J. Chem. Phys.* **113**, 297 (2000).
- [3] M. Kaern, W.J. Blake, J.J. Collins, *Annu. Rev. Biomed. Eng.* **5**, 179 (2003).

- [4] J. Paulsson, O.G. Berg, M. Ehrenberg, *Proc. Natl. Acad. Sci.* **97**, 7148 (2000).
- [5] C.V. Rao, D.M. Wolf, A.P. Arkin, *Nature* **420**, 231 (2002).
- [6] R.D. Astumian, P. Hänggi, *Phys. Today* **11**, 33 (2002); R.D. Astumian, *Science* **276**, 917 (1997).
- [7] A. Fuliński, *Chaos* **8**, 549 (1998).
- [8] N. Agmon, *J. Phys. Chem.* **B104**, 7830 (2000).
- [9] J.R. Pomeroy, E.D. Sontag, J.E. Ferrel, *Nature Cell Biology* **5**, 346 (2003).
- [10] M. Thattai, A. Van Oudenaarden, *Biophys. J.* **82**, 2943 (2002).
- [11] K.O. Alper, M. Singla, J.L. Stone, C.K. Bagdassarian, *Protein Science* **10**, 1319 (2001).
- [12] J.M.R. Parrondo, B.J. De Cisneros, *Appl. Phys.* **A75**, 179 (2002).
- [13] J. Elf, M. Ehrenberg, *Genome Research* **13**, 2475 (2003).
- [14] J. Paulsson, *Nature* **427**, 415 (2004).
- [15] J.A. White, J.T. Rubinstein, A.R. Kay, *Trends Neurosci.* **23**, 131 (2000).
- [16] C. Allen, C.F. Stevens, *Proc. Natl. Acad. Sci.* **91**, 10380 (1994).
- [17] A. van Oudenaarden, J.A. Theriot, *Nature Cell Biol.* **1**, 493 (1999).
- [18] S.M. Simon, C.S. Peskin, G.F. Oster, *Proc. Natl. Acad. Sci.* **89**, 3770 (1992).
- [19] I. Prigogine, R. Lefever, *Comp. Biochem. Physiol.* **67B**, 389 (1980).
- [20] R. Garay, R. Lefever, *J. Theor. Biol.* **73**, 417 (1978).
- [21] R. Lefever, W. Horsthemke, *Bull. Math. Biol.* **41**, 469 (1979).
- [22] C.R. Doering, J.C. Gadoua, *Phys. Rev. Lett.* **69**, 2318 (1992).
- [23] M. Bier, R.D. Astumian, *Phys. Rev. Lett.* **71**, 1649 (1993).
- [24] P. Pechukas, P. Hanggi, *Phys. Rev. Lett.* **73**, 2772 (1994); P. Reimann, *Phys. Rev. Lett.* **74**, 4576 (1995).
- [25] M. Marchi, F. Marchesoni, L. Gammaitoni, E. Menichella-Saetta, S. Santucci, *Phys. Rev.* **E54**, 3479 (1996).
- [26] A.L. Pankratov, M. Salerno, *Phys. Rev.* **E61**, 1206 (2000).
- [27] J. Iwaniszewski, *Phys. Rev.* **E54**, 3173 (1996).
- [28] M. Boguñá, J.M. Porra, J. Masoliver, K. Lindenberg, *Phys. Rev.* **E57**, 3990 (1998).
- [29] P. Reimann, R. Bartussek, P. Hänggi, *Chem. Phys.* **235**, 11 (1998).
- [30] M. Bier, I. Derenyi, M. Kostur, D. Astumian, *Phys. Rev.* **E59**, 6422 (1999).
- [31] R.N. Mantegna, B. Spagnolo, *Phys. Rev. Lett.* **84**, 3025 (2000); *J. Phys. IV (France)* **8**, 247 (1998).
- [32] B. Dybiec, E. Gudowska-Nowak, *Phys. Rev.* **E66**, 026123 (2002).
- [33] A. Ochab-Marcinek, E. Gudowska-Nowak, *Physica A* **343**, 547 (2004).
- [34] R.N. Mantegna, B. Spagnolo, *Phys. Rev. Lett.* **76**, 563 (1996).
- [35] N.V. Agudov, B. Spagnolo, *Phys. Rev.* **E64**, 035102(R) (2001).
- [36] N.V. Agudov, A.A. Dubkov, B. Spagnolo, *Physica A* **325**, 144 (2003); A. Fiasconaro, D. Valenti, B. Spagnolo, *Physica A* **325**, 136 (2003).

- [37] B. Spagnolo, A.A. Dubkov, N.V. Agudov, *Acta Phys. Pol.* **35**, 1419 (2004).
- [38] A.A. Dubkov, N.V. Agudov, B. Spagnolo, *Phys. Rev.* **E69**, 061103 (2004);  
B. Spagnolo, A. A. Dubkov, N.V. Agudov, *Eur. Phys. J.* **B40**, 273 (2004).
- [39] A.L. Pankratov, B. Spagnolo, *Phys. Rev. Lett.* **93**, 177001 (2004).
- [40] E.V. Pankratova, A.V. Polovinkin, B. Spagnolo, *Phys. Lett.* **A344**, 43 (2005).
- [41] A. Fiasconaro, B. Spagnolo, S. Boccaletti, *Phys. Rev.* **E72**, 061110(5) (2005).
- [42] W. Horsthemke, R. Lefever: *Noise-Induced Transitions. Theory and Applications in Physics, Chemistry and Biology* (Springer-Verlag, Berlin 1984).
- [43] A. Fiasconaro, B. Spagnolo, A. Ochab-Marcinek, E. Gudowska-Nowak *Noise Driven Enzymatic Reactions: Resonant Activation and Noise Enhanced Stability*, submitted to *Phys. Rev.* **E**.
- [44] P. Hänggi, P. Talkner, M. Borkovec, *Rev. Mod. Phys.* **62**, 251 (1990).
- [45] W. Sontag, *Int. J. Radiat. Biol.* **71**, 129 (1997).
- [46] H.P. de Vladar, J.A. González, *J. Theor. Biol.* **227**, 335 (2004).
- [47] G. Steel, *Basic Clinical Radiobiology*, Edward Arnold Publisher Inc., London 2002.